HIGH SCHOOL EDITION
Journal of Student Research
Volume 13 Issue 1 (2024)

The Epigenetics of Cocaine Addiction: An Analysis of D1 and D2 Dopamine Receptor-Expressing Neurons

Daniel Lee

Fieldston School, USA

ABSTRACT

Cocaine addiction is one of the most common substance use disorders worldwide. Currently, there are no medications approved by the U.S. Food and Drug Administration to treat cocaine addiction. Repeated exposure to cocaine induces long-term changes in the brain, resulting in increased displeasure and negative moods when not taking the drug. Cocaine abuse causes persistent plasticity, altering the composition and levels of membrane receptors involved in neuronal signaling pathways. This leads to long-term, stable changes in synaptic connectivity and strength in the dopaminergic system, particularly involving the D1 and D2 Dopamine Receptor-Expressing Neurons [DRD1 and DRD2]. These two cell types comprise 95% of the NAc, a key node of the brain's reward circuitry whose role is to translate motivation into action. Previously, there have been limited systematic or quantitative studies on the differences in structure between DRD1 and DRD2 neurons in the context of drug addiction. This paper mapped out the 3D structure of the DRD1 and DRD2 genome, identified the regions most affected by the epigenetic mechanisms of cocaine treatment, and quantified the subsequent changes in gene expression. Future experiments and studies can expand upon the results from this research to target specific regions of chromatin in DRD1 and DRD2 neurons in order to reverse the effects of cocaine abuse.

Introduction

Cocaine addiction is one of the most common substance use disorders worldwide. In 2021, it was estimated that roughly 24,486 people died due to a cocaine overdose (Centers for Disease Control and Prevention [CDC], 2021). Currently, there are no medications approved by the U.S. Food and Drug Administration to treat cocaine addiction. Repeated exposure to cocaine induces long-term changes in the brain, leading to increased displeasure and negative moods when not taking the drug. Overtime, the user begins to develop increased tolerance to cocaine, such that higher doses of the drug are needed to produce the same amount of pleasure and relief experienced initially (National Institute on Drug Abuse [NIDA], 2021). Simultaneously, the user may also develop sensitization to cocaine, in which lower doses are needed to produce anxiety or other toxic effects. These two factors combined increase the risk of overdose in a regular user.

One region of focus is the nucleus accumbens (NAc), part of the ventral striatum, which is responsible for the integration of information through the coordination of the cellular response to dopamine and glutamatergic inputs from several reward-associated cortical and thalamic regions in the brain. The NAc is primarily composed of medium spiny neurons (MSNs), characterized by their expression of either DRD1 (D1) or DRD2 (D2) dopamine receptors (Drds). Both Drds are G protein-coupled receptors that either activate (G_s for D1) or inhibit (G_i for D2) cyclic AMP and protein kinase A (PKA), leading to the activation (D1) or inhibition (D2) of DA-sensitive cells in the NAc (Mews et al., 2018).

Cocaine enhances neurotransmissions in the dopaminergic system by inhibiting the dopamine transporter, blocking dopamine uptake and prolonging the duration of dopamine in the extracellular space. Cocaine has also been shown to augment dopamine release, increasing dopaminergic transmission from VTA dopamine neurons (DA) into the striatum (Venton et al., 2006; Mews et al., 2018). Elevated levels of dopamine binding to its receptors activates second messenger pathways that influence transcription within the cell through a series of signaling cascades that contribute to increased sensitivity to cocaine. This occurs via the activation of calcium pathways upon receptor stimulation that transmit circuit activity to the cell nucleus. The induction of particular genes results in the activation or inhibition of many transcription factors and nuclear targets, including chromatin-regulatory proteins, which control acute and transient gene expression in response to upstream neural activity (Mews et al., 2018). This alters the composition and levels of membrane receptors involved in neuronal signaling pathways, leading to long-term, stable changes in synaptic connectivity and strength that promote continued drug use.

Chromatin-based mechanisms are the focal point of transcriptional gene regulation; activity-dependent, transient changes in chromatin structure and gene expression form the foundation for long-term epigenetic adaptations (Mews et al., 2018). These include posttranslational modifications of both histone proteins and of the DNA itself, which results in altered epigenetic signatures — i.e. heritable changes in DNA — of specific genes with crucial functions in synaptic remodeling (Mews et al., 2018).

Chromatin is organized into spatial domains known as TADs (topologically associating domains) — a fundamental structural and regulatory unit of the genome — that are characterized by their preferential contacts between loci within the same TAD (Hansen et al., 2018; Grubert et al., 2020). These regions regulate gene expression by controlling enhancer-promoter contacts. Similarly, the looping of nucleosome-containing fibers also brings specific regions of chromatin within close proximity, further influencing gene expression (Kadauke & Blobel, 2009). Highly compacted chromatin is not accessible to enzymes involved in DNA transcription or replication, whereas less condensed chromatin is typically where active transcription can take place. In other words, only by unraveling compacted chromatin can the DNA of a specific gene be made accessible to transcription.

This research aimed to determine the epigenetic effects of cocaine addiction by exploring differential interactions (DIs) between chromatin in DRD1 and DRD2 neurons, factoring in differentially expressed genes (DEGs) as part of a multi-omic approach to analyze the epigenome. The results shed light on the mechanisms of cocaine addiction, potentially leading to more effective drug treatments.

Methods

Experimental Animals

Male double-transgenic mice expressing D1 or D2-specific nuclear-tagged GFP were generated via crossing Rpl10a-GFP mice with either D1-Cre (MGI:3836633) 457 or D2-Cre (MGI:3836635) mice, obtained from The Jackson Laboratory. Mice were bred in-house on a C57BL/6J background and were between 8-20 weeks old at the beginning of the experiment. Housing was conducted on a regular light-dark cycle with lights on at 7:00am, and food and water were available as needed. The experiment was conducted in accordance with guidelines of the Institutional Animal Care and Use Committee (IACUC) at Mount Sinai.

Drug Treatment

Cocaine hydrochloride obtained from the National Institute on Drug Abuse was dissolved in 0.9% saline and administered intraperitoneally at 20 mg/kg. This dosage was chosen based on their roughly equivalent rewarding effects, established by prior conditioned place preference experiments (Godino et al., 2023).

Treatment Groups

Mice were divided into two cohorts: D1 and D2 (24 mice each). Each cohort was divided into four treatment groups of six mice each:

1. Chronic Saline + Saline Challenge (SS)
2. Chronic Saline + Cocaine Challenge (SC)
3. Chronic Cocaine + Saline Challenge (CS)
4. Chronic Cocaine + Cocaine Challenge (CC)

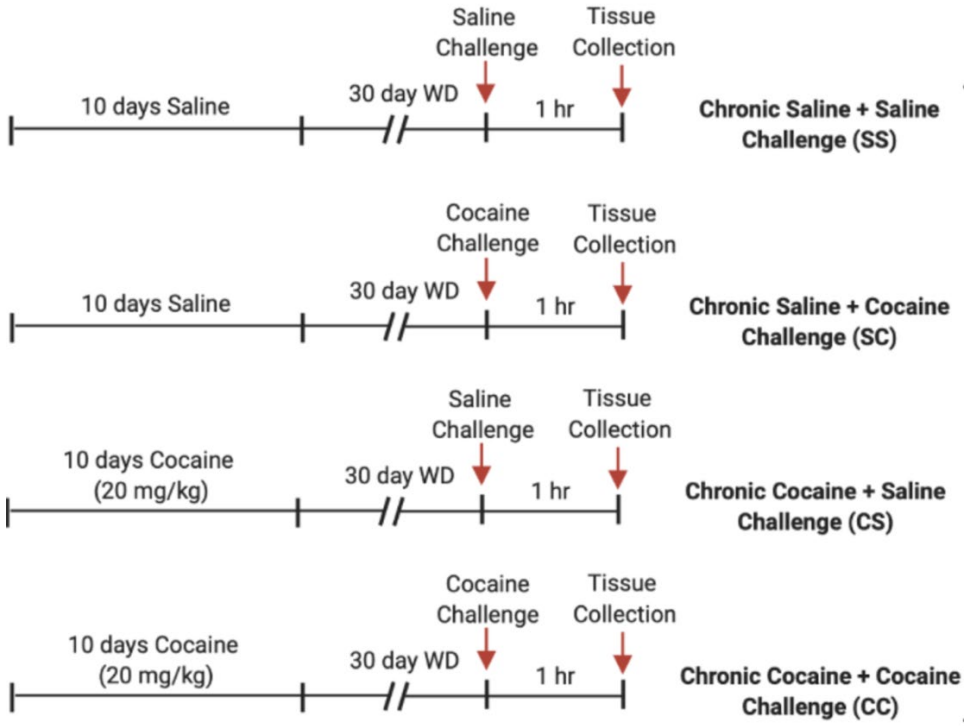

Figure 1. Summary of Cocaine Treatment Groups. Mice were injected for 10 days with 20 mg/kg of cocaine or saline, followed by a 30-day withdrawal period, and then a challenge with cocaine or saline. Mice were sacrificed one hour later.

Tissue Processing and Fluorescence Activated Nuclei Sorting (FANS)

Tissue was processed as described previously (Browne et al., 2023). Briefly, mice were euthanized by cervical dislocation. Bilateral NAc tissue was rapidly dissected on ice from 1-mm thick coronal sections using a 14G punch and flash frozen on dry ice, and nuclei were purified. Frozen NAc samples were first homogenized in

lysis buffer (0.32 M sucrose, 5 mM $CaCl_2$, 3 mM $Mg(Ace)_2$, 0.1 mM EDTA, 10 mM Tris-HCl) using high-clearance followed by low-clearance glass douncers (Kimble Kontes). Homogenates were then passed through a 40um cell strainer (Pulriselect) into ultracentrifuge tubes (Beckman Coulter). A 5ml high-sucrose cushion (1.8 M sucrose, 3 mM $Mg(Ace)_2$, 1 mM DTT, 10 mM Tris-HCl) was underlaid, and samples were centrifuged at 24,000 rpm at 4°C for 1h in a SW41Ti Swinging-Bucket Rotor (Beckman Coulter). After discarding the supernatant, nuclei pellets were resuspended in 500µl of ice-cold phosphate-buffered saline, and DAPI (1:5000) was added. All solutions contained inhibitors for RNAse (SUPERase-in, Invitrogen) and ribonuclease (RNasin Recombinant, Promega) at concentrations of 1:1000 (sucrose buffer) or 1:500 (lysis buffer and PBS). Nuclei were then immediately sorted using a BD FACS Aria II three-laser system with a 100µm nozzle. Debris and doublets were first gated based on forward scatter and side scatter. Nuclei were then gated as DAPI-positive events (Violet1-A laser), and GFP positive events were sorted directly into 1.5 ml Eppendorf tubes containing TriZol LS (Ambion) and flash frozen on dry ice for RNA sequencing or sorted into 1X PBS for genome-wide HiC (described below). Samples ranged from 18,000-60,000 GFP+ nuclei collected for both downstream analyses.

RNA-Sequencing

After FANS, nuclei were thawed on ice and homogenized in TriZol, and RNA was extracted using the Direct-zol RNA microprep kit (Zymo Research) according to manufacturer instructions. To generate sequencing libraries, 1ng of total RNA was used as input for Takara SMARTer® Stranded Total RNA-Seq Kit v3 - Pico Input Mammalian kit, with ribodepletion, according to manufacturer's instructions. Sequencing libraries were generated for each sample individually using Takara's Unique Dual Index Kit. Following library preparation, sequencing was performed with Genewiz/Azenta on an Illumina Novaseq S4 machine with a 2x150 bp paired-end read configuration producing 40M reads per sample. All samples were multiplexed and run concurrently. Quality control was performed using FastQC (www.bioinformatics.babraham.ac.uk/projects/fastqc/). All raw sequencing reads underwent adapter trimming using Trimmomatic (github.com/usadellab/Trimmomatic) and were mapped to mm10 using HISAT2 (daehwankimlab.github.io/hisat2/). Duplicate reads were removed using Picard MarkDuplicate tool (broadinstitute.github.io/picard/), and count matrices were generated using the featureCounts function of the subread package (subread.sourceforge.net/featureCounts.ht).

Steps for HiC Data Collection

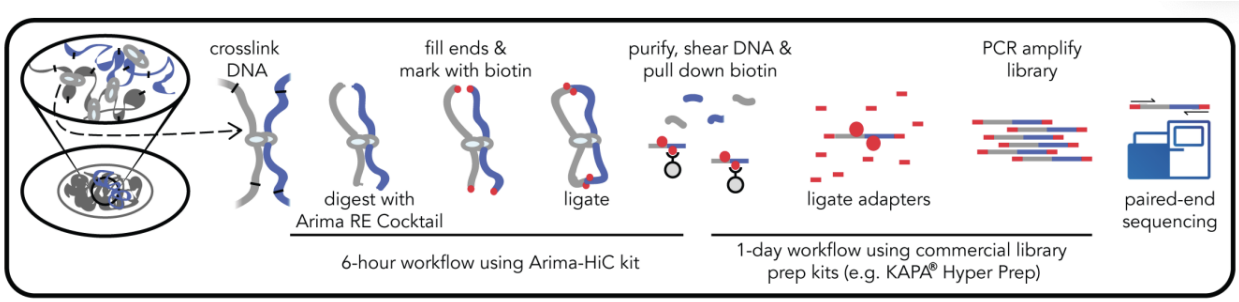

Figure 2. Arima-HiC Workflow Overview (Arima Genomics, 2019).

Step 1: Crosslinking and DNA fragmentation

1.1 HiC Pre-Prep: Protocol was conducted in accordance with the Arima HiC Kit (Arima Genomics, 2021). Nuclei was sorted into 1X PBS. Volume of 1X PBS was brought up to 5 mL. Next, 286µL of 37% formaldehyde

was added, bringing the final formaldehyde concentration to 2%. Samples were inverted 10 times and incubated at RT for 10 min. 460µL of Arima HiC Kit's 'Stop Solution 1' was added. Samples were inverted 10 times and incubated at RT for 10 min. Samples were placed on ice and incubated for 15 min. Samples were pelleted by centrifugation. Supernatant was discarded. Cells were resuspended in 5mL 1X PBS. Samples were aliquoted into several new tubes, with 1 x 106 cells per aliquot. Samples were mixed by inversion between aliquots to ensure all aliquots were equally homogeneous. Cells were pelleted in all aliquots by centrifugation. Supernatant was discarded leaving only the crosslinked cell pellet and no residual liquid. Samples were frozen on dry ice or liquid nitrogen, and stored at -80°C (Arima Genomics, 2021).

1.2 Arima-HiC Quick Reference Protocol: Protocol was conducted in accordance with the Arima HiC Kit (Arima Genomics, 2021). Nuclei were then resuspended in 20 µL water, and incubated for 15 min at 4 ºC. 24 µL of *Conditioning Solution* from the Arima-HiC+ Kit was added. Samples were incubated for 10 min at 62 ºC. 24 µL of *Stop Solution 2* was added. Samples were incubated for 15 min at 37 ºC. 7 µL of *Buffer A*, 1 µL of *Enzyme A1*, and 4 µL of Enzyme A2 were added. Samples were incubated for 30 min at 37 ºC followed by 20 min at 62 ºC. 12 µL of *Buffer B* and 4 µL of *Enzyme B* were added. Samples were incubated for 45 min at 25 ºC. 70 µL of *Buffer C* and 12 µL of *Enzyme C* were added. Samples were incubated for 15 min at 25 ºC. 10.5 µL of *Buffer D*, 25 µL of *Enzyme D*, and 20 µL of Buffer E were added. Samples were incubated for 30 min at 55ºC followed by 90 min at 68ºC. QC was conducted on Agilent Tapestation to assess DNA fragmentation size and concentration to confirm an appropriate fragment size distribution centered around 400 bp.

Step 2. Library Preparation

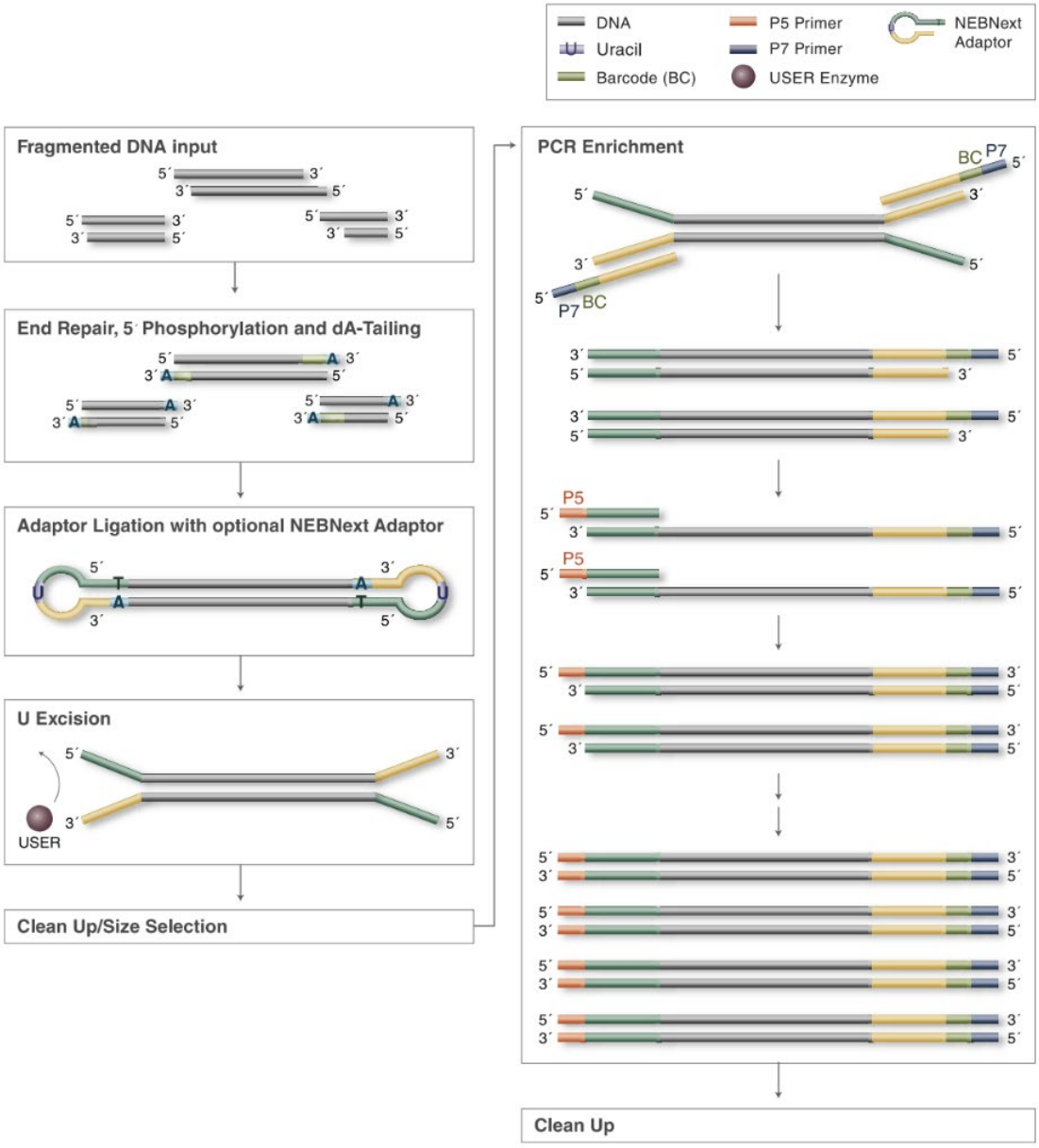

Figure 3. Workflow Overview of Library Prep Kit for Illumina (New England BioLabs, 2022).

2.1 DNA Size Selection: Protocol was conducted in accordance with the Arima Library Prep Module (Arima Genomics, 2023). Fragmented DNA samples were transferred from fragmentation tube to microfuge tube. Elution buffer was added to bring each sample's volume to 100 µL. 60 µL of DNA Purification Beads (AMPure XP Beads) were added and mixed thoroughly by pipetting. Samples were incubated at RT for 5 min. Samples were placed against the magnet and incubated until the solution was clear. 160 µL of supernatant from each sample was transferred to a new sample tube. Beads were discarded. 40 µL of DNA Purification Beads were added to the supernatant and mixed thoroughly by pipetting. Samples were incubated at RT for 5 min. Samples were placed against the magnet and incubated until the solution was clear. Supernatant was discarded. While samples were still against the magnet, 200 µL of 80% ethanol was added and incubated at RT for 1 min. Repeat the previous two steps. Supernatant was discarded. While samples were still against the magnet, beads were

incubated at RT for 1 min to air-dry. Samples were removed from the magnet. Beads were resuspended in 30 µL of Elution Buffer and incubated at RT for 5 min. Samples were placed against the magnet, incubated until solution was clear, and supernatant was transferred to a new sample tube. Samples were quantified using Qubit.

2.2 Biotin Enrichment: Protocol was conducted in accordance with the Arima Library Prep Module (Arima Genomics, 2023). *T1 Beads* from the Arima-HiC+ Kit were mixed and prepared. 12.5 µL of *T1 Beads* were placed into a well of a strip tube for each sample. *T1 Beads* were washed in each tube by the following steps: Adding 200 µL of *Binding Buffer*, mixing by pipetting up and down 20 times, capping the tubes, vortexing at high speeds for 5-10 seconds, placing tubes against a magnet and incubating for 5 minutes, discarding supernatant and removing tube from magnet, repeating the previous steps two more times, resuspending beads in 200 µL of *Binding Buffer*, transferring 200 ng of size-selected DNA into a new microfuge tube, and adding Elution buffer to bring sample volume to 30 µL. Next, 200 µL of washed *T1 Beads* were added in *Binding Buffer*, mixed thoroughly by pipetting and incubated at RT for 5 min. The following steps were repeated twice: Wash beads by resuspending in 200 µL of *Wash Buffer* and incubate at 55°C for 2 min; set lid temperature to 85°C; place samples against magnet and incubate until solution is clear; discard supernatant and remove samples from magnet. Next, beads were washed by resuspending in 100 µL of Elution Buffer. Samples were placed against the magnet and incubated until the solution was clear. Supernatant was discarded and samples were removed from the magnet. Beads were resuspended in 50 µL of Deionized / Nuclease-free Water.

2.3 Library Preparation of Enriched Ligation Products: 20 µL of the *End Repair* and *dA-Tailing* master mix from the Arima-HiC+ Kit was added to each sample containing 50 µL of Bead bound HiC library from the previous section. Samples were placed into the thermal cycler for 15 min at 20 ºC, 15 min at 72 ºC, and held at 4 ºC. Next, samples were transferred to ice while preparing the ligation reaction. 25µL of *Ligation Master Mix* from the previous step was added to the 70µL of bead bound, end repaired and dA-tailed HiC library. 5µL of *Adaptor Oligo Mix* was added to each sample. Tubes were spun briefly and placed into the thermal cycler for 30 min at 20 ºC and held at 4 ºC. Samples were removed from the thermocycler and spun to remove liquid from the caps. Beads were magnetized until liquid was clear. Supernatant was discarded. Beads were resuspended in 200µL Wash Buffer and mixed by pipetting. Samples were incubated at 55 ºC for 2 min. Lid temperature was set to 85°C. Beads were magnetized until liquid was clear. Supernatant was discarded. Beads were resuspended in 100µL Elution Buffer. Beads were magnetized until liquid was clear. Supernatant was discarded.

Beads were resuspended in 34µL of Deionized Water. 11µL of the *PCR reaction mixture* from the Arima-HiC+ Kit was added to the 34 µL of *Adaptor Ligated Bead Bound HiC Library* from the previous step. 5uL of the appropriate, unique, *Index Primer Pair* was added to each sample. Samples were placed in the thermal cycler for 1X at 98ºC for 2 min, 12X of (98 ºC for 30 sec, 60 ºC for 30 sec, and 72 ºC for 1 min), 1X 72 ºC for 5 min, and held at 4ºC. 50 µL of DNA Purification Beads was added to each 50 µL Indexed sample, and incubate for 5 min at RT. Samples were placed against the magnet and incubated until the solution was clear. Supernatant was discarded. While samples were still against the magnet, 200µL of 80% ethanol was added, and incubated at RT for 1 min. Supernatant was discarded. The previous two steps were then repeated. Next, supernatant was discarded. While samples were still against the magnet, beads were incubated at RT for 3 – 5 min to air-dry. Samples were removed from the magnet, and beads were resuspended in 15µL of Deionized / Nuclease-free Water, incubated at RT for 5 min. Samples were placed against the magnet and incubated until the solution was clear. Purified and complete HiC libraries were removed and transferred to a fresh PCR strip tube. Samples were quantified using Qubit using 1 µL to determine the size and distribution of the HiC library.

HiC Data Processing

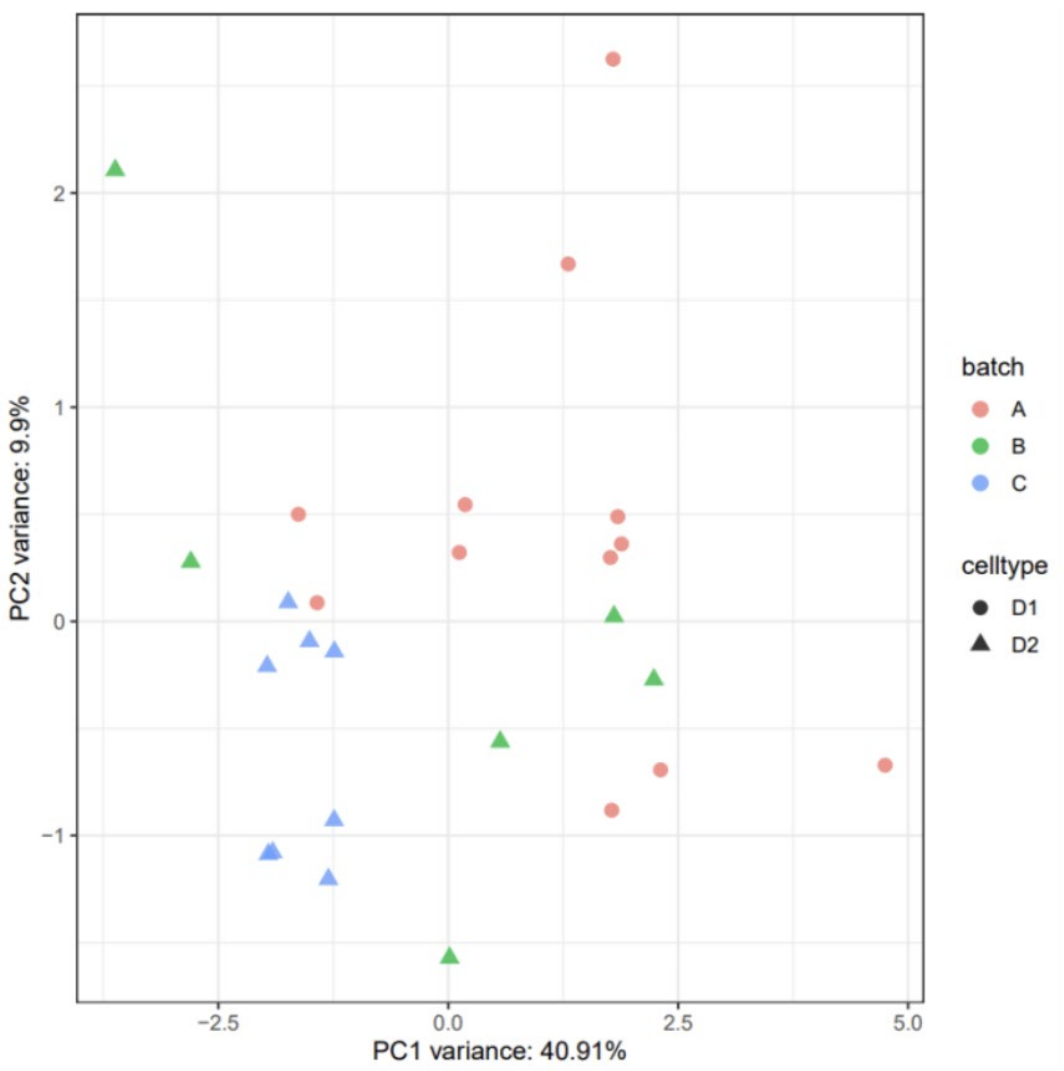

Figure 4. PCA (Principal Component Analysis) plot was created for pooled samples in each treatment group. After the removal of six outliers in the D2 samples, the PCA plot above was generated, showing that the data was randomly distributed across PC1 and PC2 variance.

The remaining samples were examined for various quality metrics and were determined to be consistent with the recommended ranges from ENCODE (shown in Figure 5). As a sample metric, the duplication rates are shown in Figure 6.

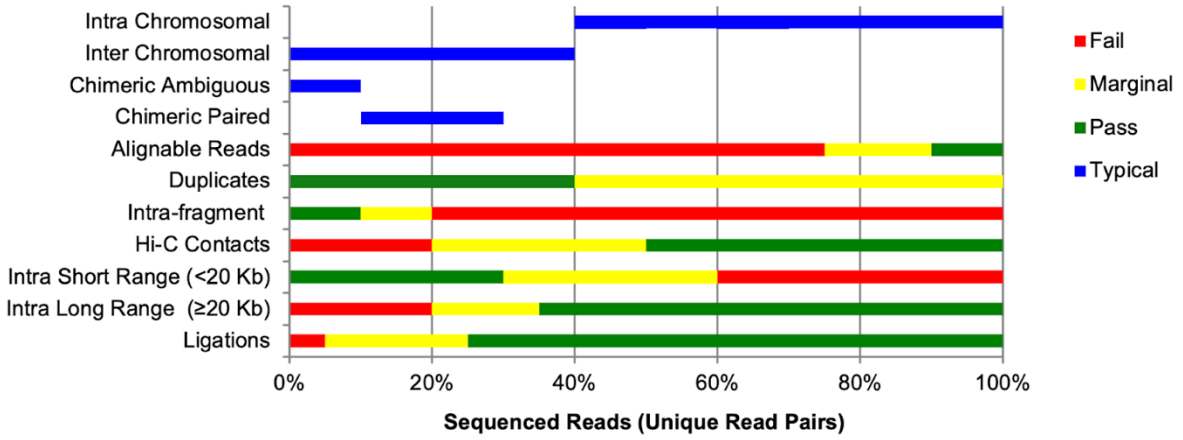

Figure 5. Hi-C Library Statistic Standard Thresholds for Passing, Failing, and Marginal (The Encyclopedia of DNA Elements [ENCODE], 2018).

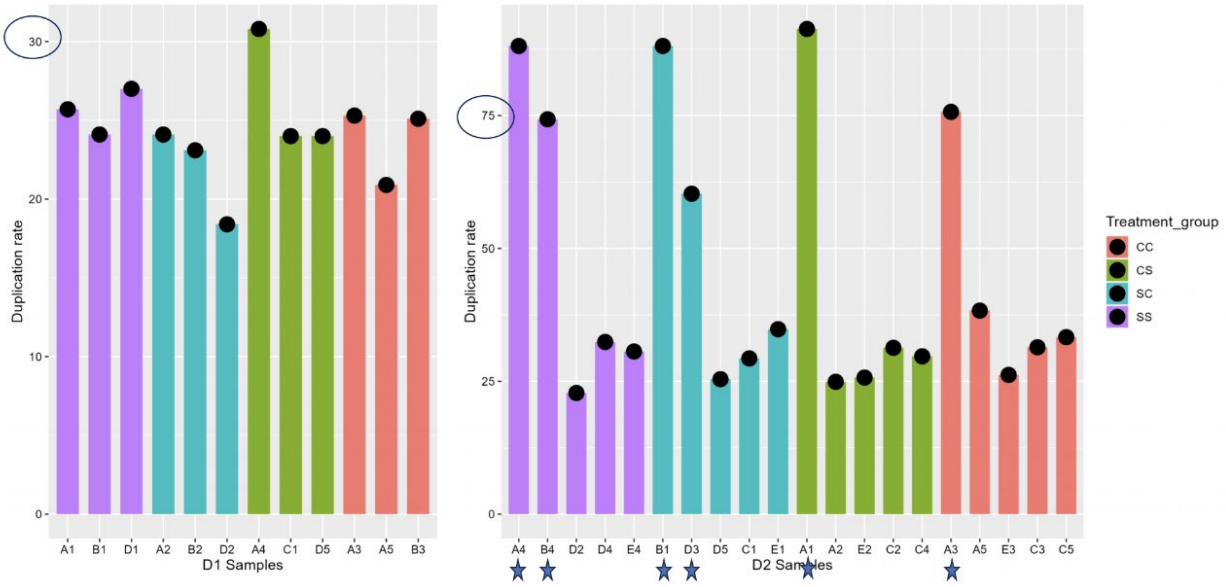

Figure 6. Duplication Rates of Individual Samples. Outliers are indicated by the blue stars, and fall outside the recommended ranges by ENCODE.

Juicertool's *Arrowhead* and *Hiccups* software were used to detect the TADs and loops, respectively, for each treatment group, at 10kb, 25kb, and 50kb resolution.

Differential interactions were determined using *HiCDC*, and differential gene analysis was conducted using *DESeq2*. Both softwares were filtered for a significance threshold of $p < 0.01$ and $|log_2 foldchange| > 0.3$ in order for a given region or feature to be considered differential. Fold Change indicates the magnitude of the change in gene expression or chromatin interaction; a more positive Fold Change means the sample measure was greater in DRD1 neurons, while a negative Fold Change indicates that the measure was greater in DRD2 neurons.

Next, D1 and D2 samples were pooled together, allowing us to improve coverage for D1/D2 cell types. The *Juicebox* program from Aidenlab was used to create visualizations of the pooled HiC data.

Using a program in R, the cell-type specific genomic features were merged together across multiple resolutions (10kb, 25kb, and 50kb) for both D1/D2 groups to form a union list of TADs and loops. This method 'merged' together all TADs that shared at least 70% of their chromatin area, taking the largest possible area covered by two TADs.

HiCExplorer's *hicPlotTADs* program was used to generate visualizations of these genomic features for comparison between D1 / D2 cell types.

The TADs and loops were then overlapped with the differential interactions and differentially-expressed genes using a program in R with the GenomicRanges library. This involved several steps: overlapping the TADs with the mouse gene promoters, obtaining the corresponding gene symbols, and filtering the list for DEGs from the individual treatment groups and the differential interactions between D1 and D2.

Results

Section 1: Detecting TADs and Loops to Determine Chromatin Structure

A large magnitude of epigenetic changes in both DRD1 and DRD2 neurons was observed due to different patterns of cocaine usage. Section 1 reveals variations in both the total number and median size of TADs and loops in DRD1 and DRD2 neurons of mice in different cocaine treatments. Table 1 and Table 2 show the total number of TADs and median length of TADs in the DRD1 and DRD2 genomes of mice from each treatment group, respectively. Table 3 and Table 4 show the total number of loops and median length of loops in the DRD1 and DRD2 genomes of mice from each treatment group, respectively.

Table 1. Number of TADs Detected in the DRD1 and DRD2 Genomes of Mice from Each Treatment Group.

	D1_SS	D1_SC	D1_CS	D1_CC	D2_SS	D2_SC	D2_CS	D2_CC
10kb resolution	3,048	2,223	3,740	2,710	3,544	3,677	4,590	4,236
25kb resolution	3,166	2,728	3,315	3,005	3,307	3,342	3,715	3,619
50kb resolution	1,979	1,807	2,012	1,943	2,012	2,012	2,193	2,149

Column names denote the cell-type (i.e. 'D1' or 'D2') and the treatment group (SS: chronic saline + saline challenge; SC: chronic saline + cocaine challenge; CS: chronic cocaine + saline challenge; CC: chronic cocaine + cocaine challenge). Row names indicate the resolution (10kb, 25kb, and 50kb). TADs were generated using Juicertool's *Arrowhead* program with default parameters. n=3.

Table 2. Median Length of TADs Detected in the DRD1 and DRD2 Genomes of Mice from Each Treatment Group.

	D1_SS	D1_SC	D1_CS	D1_CC	D2_SS	D2_SC	D2_CS	D2_CC
10kb resolution	220,000	220,000	230,000	220,000	230,000	230,000	250,000	240,000

25kb resolution	600,000	575,000	600,000	600,000	600,000	600,000	625,000	625,000
50kb resolution	1,150,000	1,100,000	1,150,000	1,150,000	1,200,000	1,200,000	1,200,000	1,200,000

Table 3. Number of Loops Detected in the DRD1 and DRD2 Genomes of Mice from Each Treatment Group.

	D1_SS	**D1_SC**	**D1_CS**	**D1_CC**	**D2_SS**	**D2_SC**	**D2_CS**	**D2_CC**
Number of Loops	5,489	4,744	6,677	5,039	6,617	6,851	7,668	7,116

Column names denote the cell-type (i.e. 'D1' or 'D2') and the treatment group (SS: chronic saline + saline challenge; SC: chronic saline + cocaine challenge; CS: chronic cocaine + saline challenge; CC: chronic cocaine + cocaine challenge). Loops were detected using Juicertool's *Hiccups* program with default parameters at 10kb and 25kb resolution. n=3.

Table 4. Median Length of TADs Detected in the DRD1 and DRD2 Genomes of Mice from Each Treatment Group.

	D1_SS	**D1_SC**	**D1_CS**	**D1_CC**	**D2_SS**	**D2_SC**	**D2_CS**	**D2_CC**
Median Length of Loops	280,000	275,000	290,000	275,000	280,000	290,000	295,000	300,000

Section 2: A Closer Comparison Between Treatment Groups

In this section, a closer comparison between treatment groups was made. Figure 7 shows quantifiable changes in gene expression between treatment groups, most notably in CSvSC [Chronic Cocaine + Saline Challenge *versus* Chronic Saline + Cocaine Challenge], in which over 5,000 genes in DRD1 neurons and over 2,000 genes in DRD2 neurons were differentially expressed. Additionally, there are clear differences in the number of differentially expressed genes in DRD1 versus DRD2 neurons, even when comparing the same two treatment groups. For instance, while there were 3,044 differentially expressed genes in DRD1 neurons in CCvSS, there were only 49 in DRD2 neurons, suggesting a cell-type specific role in the remodeling of the dopaminergic system. This relationship is further explored in Section 3.

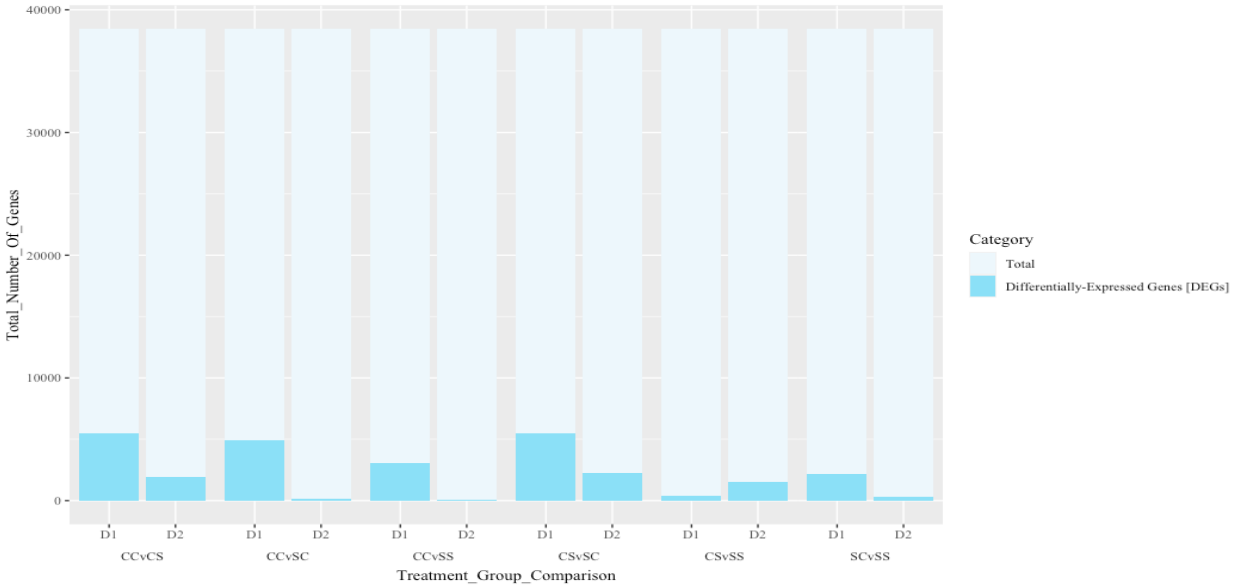

Figure 7. Differentially-Expressed Genes in Each Treatment Group Comparison. This figure shows the number of differentially-expressed genes in Drd1 and Drd2 neurons between each treatment group comparison. The total number of genes in both cells is 38,446.

Table 5. Differentially-Expressed Genes in Each Treatment Group Comparison.

Treatment Group Comparison	CCvCS		CCvSC		CCvSS		CSvSC		CSvSS		SCvSS	
Cell Type	**D1**	**D2**	**D1**	**D2**	**D1**	**D2**	**D1**	**D2**	**D1**	**D2**	**D1**	**D2**
Differentially-Expressed Genes [DEGs] (out of 38,446 total genes)	5,512	1,914	4,891	118	3,044	49	5,451	2,230	377	1,513	2,136	274

Section 3: Pooling Together D1 and D2 Cell-Types

In Section 3, the D1 and D2 data was pooled together in order to explore the cell-type specific genomic interactions between DRD1 and DRD2 neurons. Figure 8 depicts a complete 3D map of the D1 and D2 genome, showing their unique chromosomal architectures and genomic organization.

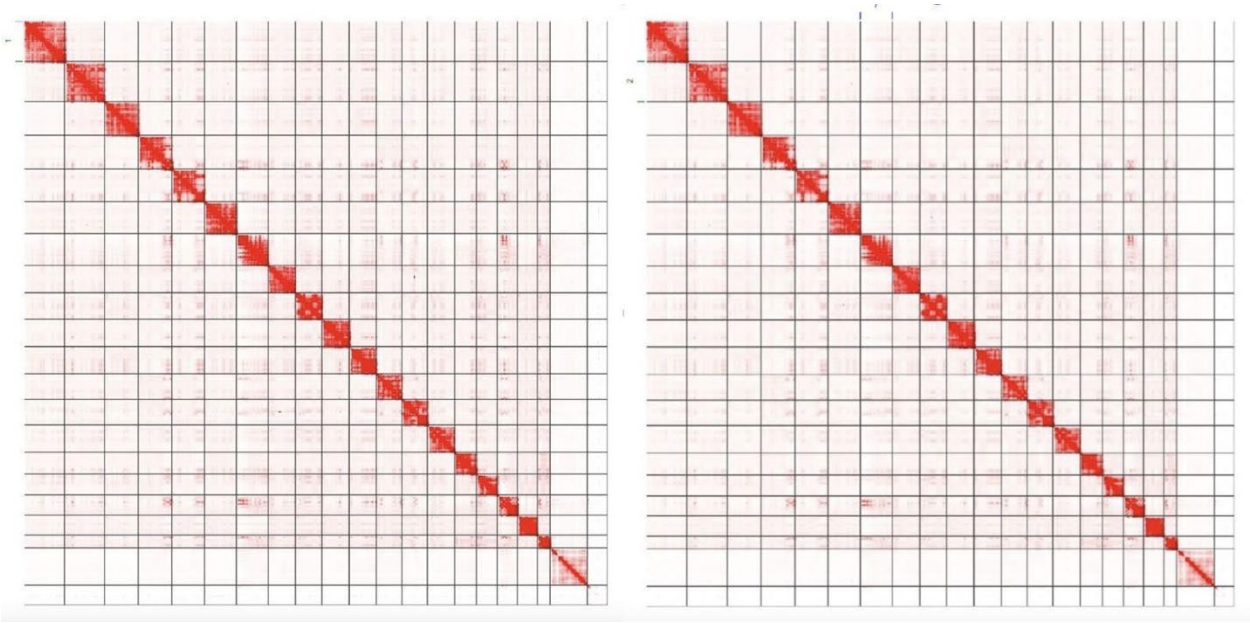

Figure 8. 3D HiC Matrices of the DRD1 and DRD2 Genomes. The figure above depicts two n-by-n matrices which indicate the frequency of interactions between different loci of chromatin in DRD1 (left) and DRD2 (right) neurons; the rows and columns of the matrix correspond to the different sets of positions in the genome. Each line represents the division between each chromosome. The lighter areas indicate regions of lower interaction, whilst the darker areas indicate regions of higher interaction. For example, the color value of the matrix at 30Mb down and 60Mb to the right represents how frequently those two loci of chromatin physically interact with each other. This visualization was created using the *Juicebox* program from Aidenlab.

Each chromosome has its own unique 3D structure, with slight, small-scale variations between cell-types. Figure 9 zooms in on chromosome 13 from Figure 8, and compares the D1 and D2 loci.

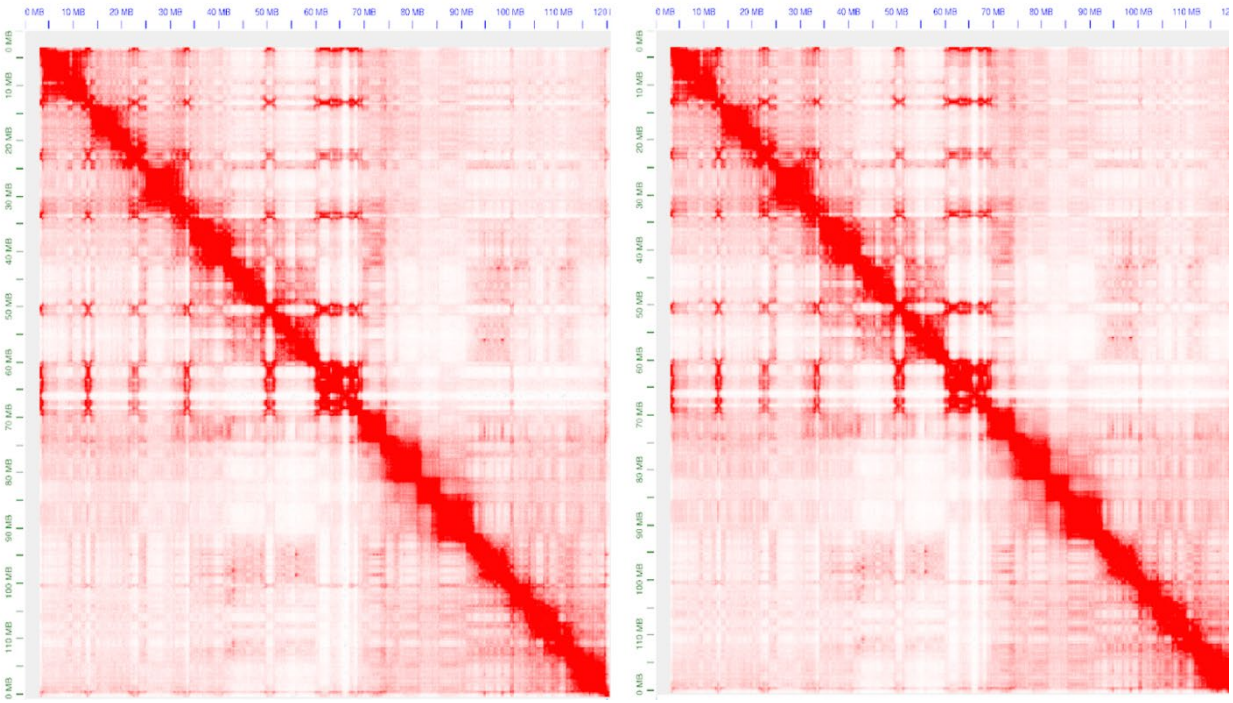

Figure 9. 3D HiC Matrices of Chromosome 13 in the DRD1 and DRD2 (right) Genomes. This figure is a zoomed-in version of Figure 8. focusing on *chromosome 13* at 500kb resolution. This visualization was created using the *Juicebox* program from Aidenlab.

To illustrate these differences in more detail, Figure 10 zooms in on chromosome 13 from position 52.0 Mb to 56.0 Mb. This study has identified the unique TAD in the DRD1 locus (shown at the bottom of Figure 10) from position 53.88 Mb to 54.09 Mb, which contains the promoter region of the *Drd1* gene that encodes for the Domaine 1 receptor. This region has been shown to contain significant differential interactions between DRD1 and DRD2 from the *HiCDC* analysis ($p = 8.32 \cdot 10^{-31}$ and $log_2 foldchange = -2.48$), meaning that this area contains far more frequent chromatin interactions in DRD1 compared to DRD2. Furthermore, the *DRD1* gene has been shown to be downregulated in the CC treatment group [Chronic Cocaine + Cocaine Challenge], possibly suggesting a decrease in the production of Dopamine 1 receptors after long-term cocaine usage.

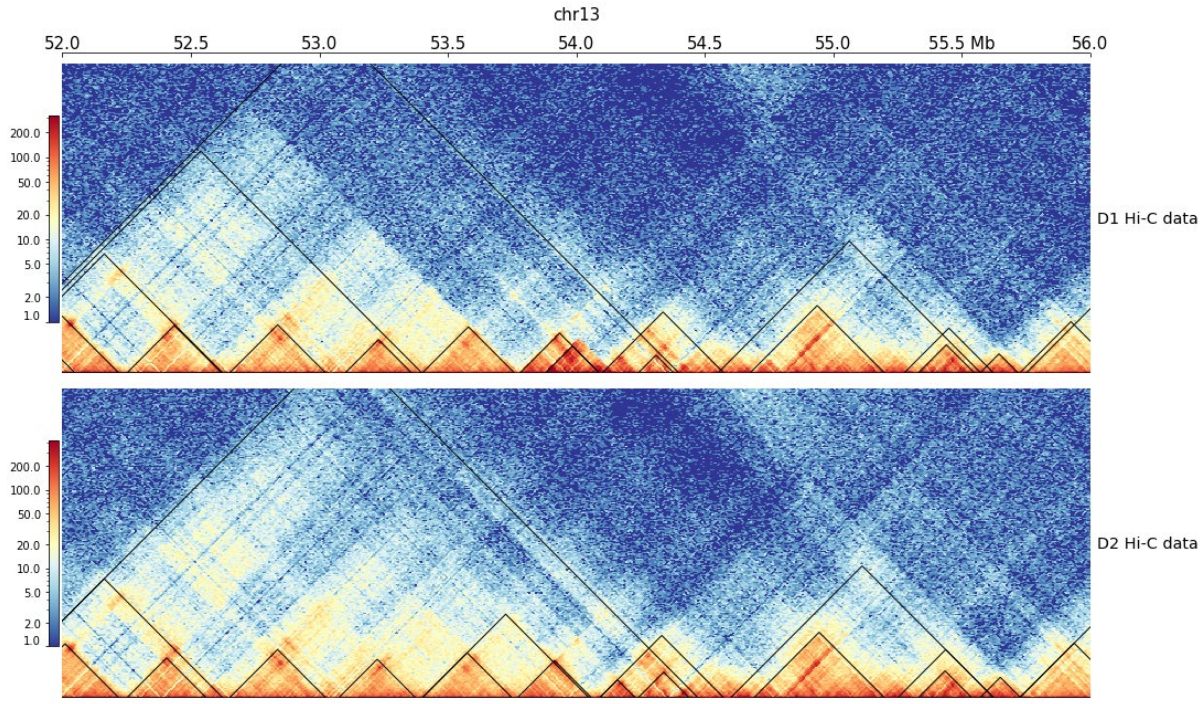

Figure 10. Differential Genomic Interactions Between DRD1 and DRD2 Cell Types. This figure compares the HiC contact matrices of the DRD1 (top) and DRD2 (bottom) genomes, focusing on a specific region within *chromosome 13* from position 52.0 Mb to 56.0 Mb. The areas colored in blue indicate regions of lower interaction, whilst the areas in red indicate regions of higher interaction; see the scale on the left side of the figure. This visualization was created using HiCExplorer's *hicPlotTADs* program. The figure depicts the upper right half of a HiC contact matrix — the x-axis represents a portion along the main diagonal in Figure 9. This allows for a closer examination of the differences in the formation of TADs (outlined in black) between D1 and D2, with a region of differential interactions indicated in the green rectangles. This area contains far more frequent chromatin interactions in DRD1 in comparison to DRD1, verified by the *HiCDC analysis*.

Likewise, the unique TAD in the DRD2 locus which contains the promoter region of the *Drd2* and *Ankk1* genes that encode for the Domaine 2 receptor has also been identified (shown at the bottom of Figure 11) as position 49.27 Mb to 49.48 Mb in chromosome 9. This region has been shown to contain significant differential interactions between DRD1 and DRD2 from the *HiCDC* analysis ($p = 8.53 \cdot 10^{-51}$ and $log_2 foldchange = 3.48$). Furthermore, both the *Drd2* and *Ankk1* genes have been shown to be upregulated in CS [Chronic Cocaine + Saline Challenge] compared to the SC treatment group [Chronic Saline + Cocaine Challenge], possibly suggesting an increase in the production of Dopamine 2 receptors in mice that received a chronic dose of cocaine and went through withdrawal compared to than an acute dose.

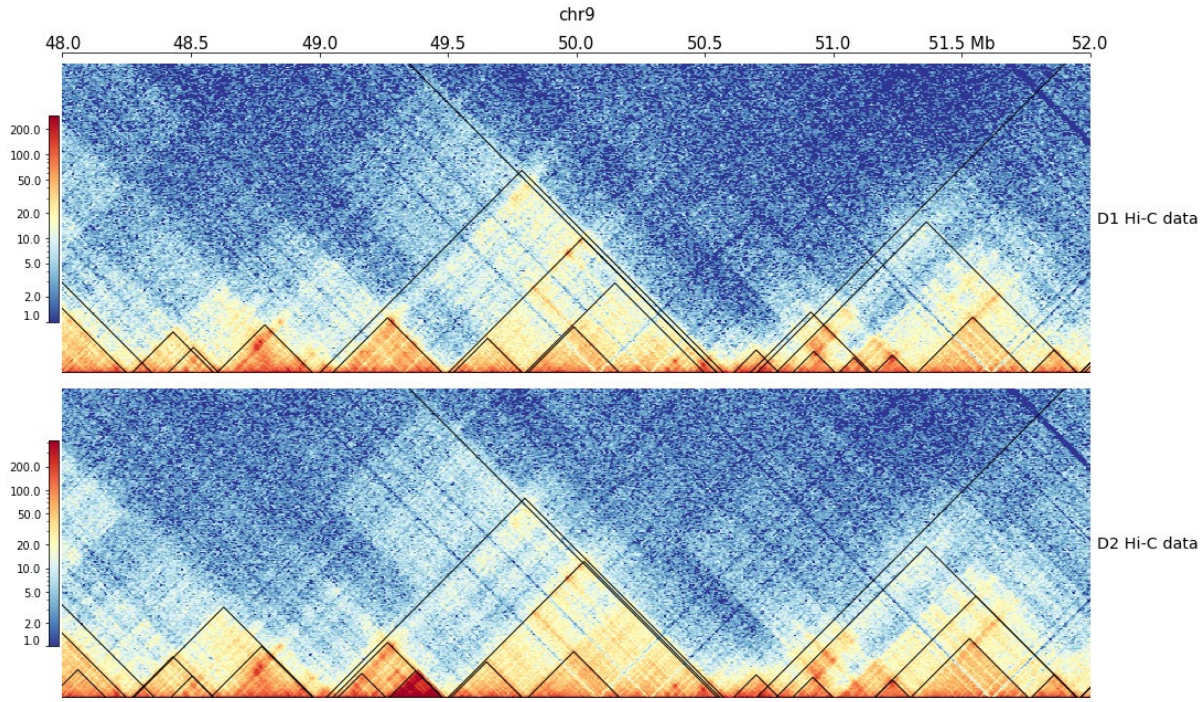

Figure 11. Differential Genomic Interactions Between DRD1 and DRD2 Cell Types. This figure compares the HiC contact matrices of the DRD1 (top) and DRD2 (bottom) genomes, focusing on a specific region within *chromosome 9* from position 48 Mb to 52 Mb. The areas colored in blue indicate regions of lower interaction, whilst the areas in red indicate regions of higher interaction; see the scale on the left side of the figure. This visualization was created using HiCExplorer's *hicPlotTADs* program. The figure depicts the upper right half of a HiC contact matrix — the x-axis represents a portion along the main diagonal in Figure 9. This allows for a closer examination of the differences in the formation of TADs (outlined in black) between D1 and D2, with a region of differential interactions indicated in the green rectangles. This area contains far more frequent chromatin interactions in DRD2 in comparison to DRD1, verified by the *HiCDC analysis*.

Collectively, this information is synthesized together in Figure 12, which shows a summary of all the differential analyses conducted in this project. The figure highlights that a significant proportion of TADs in both the DRD1 and DRD2 genomes contain not only differentially-expressed genes from each treatment group, but also differential interactions between D1 and D2; in other words, there are unique cell-type specific regions of chromatin in DRD1 and DRD2 neurons that respond differently to cocaine treatment — and the precise location and magnitude of these changes have been identified and quantified.

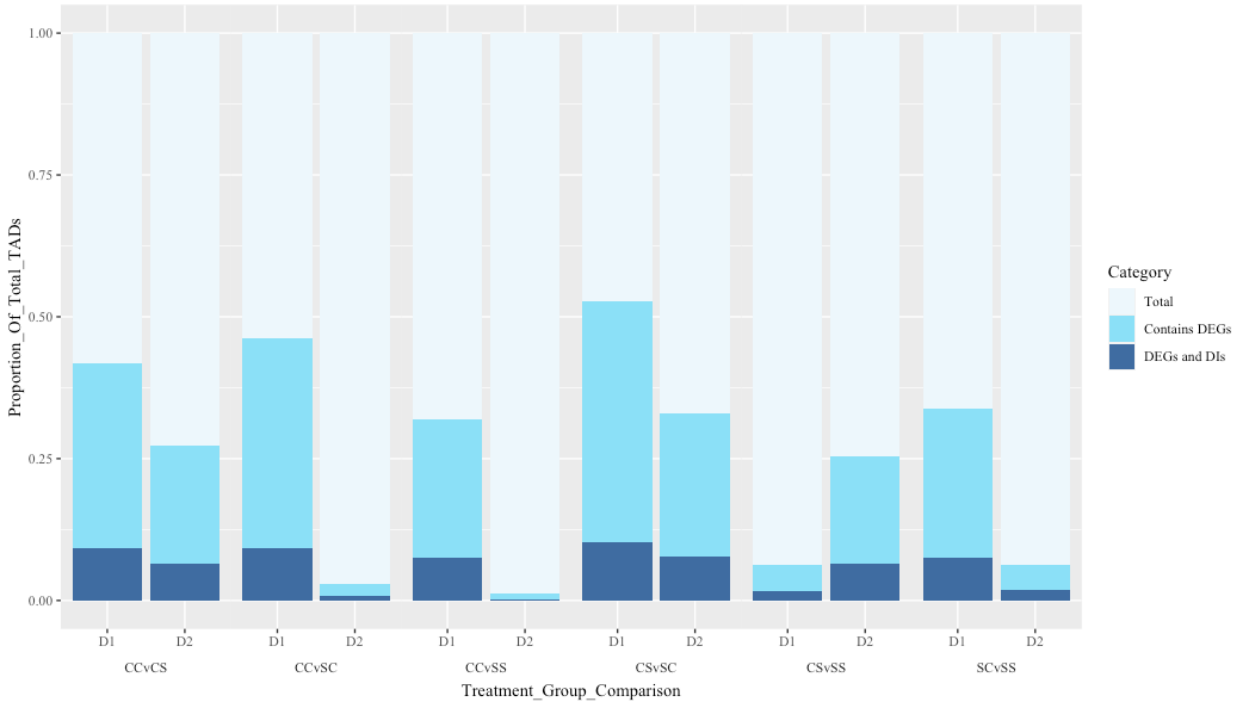

Figure 12. Summary of Differential TAD Analysis. The figure above shows the proportion of the total number of TADs (9,075 in D1 and 9,480 in D2) in the complete DRD1 and DRD2 genomes that contain either DEGs — the promoter regions of differentially-expressed genes in each of the six treatment group comparisons — or both DEGs and DIs — regions with differential interactions between D1 and D2. The DEGs were obtained from Figure 7. The DIs were calculated using HiCDC.

Table 6. Summary of Differential TAD Analysis.

Treatment Group Comparison	**CCvCS**		**CCvSC**		**CCvSS**		**CSvSC**		**CSvSS**		**SCvSS**	
Cell Type	**D1**	**D2**	**D1**	**D2**	**D1**	**D2**	**D1**	**D2**	**D1**	**D2**	**D1**	**D2**
Total Number of TADs	9,075	9,480	9,075	9,480	9,075	9,480	9,075	9,480	9,075	9,480	9,075	9,480
TADs containing DEGs	3,786	2,591	4,200	267	2,888	108	4,780	3,131	574	2,400	3,059	596
TADs containing DEGs and DIs	838	609	845	69	691	21	928	735	157	612	688	184

These results show promising paths for future research on the treatment of cocaine addiction and the reversal of drug-related epigenetic changes.

Conclusion

The purpose of this study was to determine the epigenetic effects of cocaine addiction and identify the cell-type specific genomic interactions between DRD1 and DRD2 neurons. Through the application of a novel approach synthesizing both HiC data and RNA sequencing, the location and magnitude of these epigenetic changes have been precisely identified and quantified.

By enhancing neurotransmissions in the dopaminergic system through disrupting the cycle of dopamine uptake and augmenting dopamine release, prolonged cocaine usage leads to the activation or inhibition of many chromatin-regulatory proteins, which control acute and transient gene expression. This alters the levels of membrane receptors involved in neuronal signaling pathways, leading to long-term, stable changes in synaptic connectivity and strength that promote continued drug use.

Mapping out the structure of the genome in DRD1 and DRD2 neurons, which comprise roughly 95% of the nucleus accumbens (NAc), is crucial to understanding how the brain's reward system adapts to external influences, especially drug addiction (Soares-Cunha et al., 2018). Given that DRD1 and DRD2 cells have contrasting roles in the dopaminergic system, since DRD1 neurons are excitatory while DRD2 neurons are inhibitory, changes in the levels and structure of these two types of cells leads to major behavioral abnormalities in response to drug treatment (Eagle et al., 2011). As shown in Figure 7 and Figure 12, both acute and chronic cocaine usage lead to quantifiable changes in gene expression in both DRD1 and DRD2 neurons that can be attributed to specific regions of chromatin unique to the DRD1 or DRD2 genome. Specifically, this paper has identified the precise location of the TAD in the DRD1 genome that contains the *Drd1* gene, which encodes for the Dopamine 1 receptor, and the TAD in the DRD2 genome that contains the *Drd2* and *Ankk1* genes, which encode for the Dopamine 2 receptor.

The *Drd1* gene has been shown to be downregulated after long-term cocaine usage, and the *Drd2* and *Ankk1* genes have been shown to be upregulated after chronic cocaine usage compared to acute.

Previously, there have been limited systematic or quantitative studies on the differences in structure between DRD1 and DRD2 neurons; however, this research expands the horizon in terms of potential drug-treatments to reverse the effects of cocaine. Now, future studies will have a much clearer picture of how cocaine reorganizes DRD1 and DRD2 cells in order to sustain a different functional state in which the user becomes reliant on cocaine long after the initial exposure to the drug.

Acknowledgments

I would like to thank my advisor for the valuable insight provided to me on this topic.

References

Arima Genomics. (2019, October). *Arima-HiC Kit*. https://arimagenomics.com/wp-content/files/User-Guide-Arima-HiC-for-Animal-Tissues.pdf

Arima Genomics. (2021, November). *Arima High Coverage HiC Kit*. https://arimagenomics.com/wp-content/files/User-Guide-Arima-High-Coverage-for-Mammalian-Cell-Lines.pdf

Arima Genomics. (2023, May). *Arima Library Prep Module*. https://arimagenomics.com/wp-content/files/User-Guide-Library-Preparation-using-Arima-Library-Prep-Kit.pdf

Browne, C.J., Mews, P., Zhou, X., Holt. L.M., Estill, M., Futamura, R., Schaefer, A., Kenny, P.J., Hurd, Y.L., Shen, L., Zhang, B., Nestler, E.J. (2023). Shared and divergent transcriptomic regulation in nucleus accumbens D1 and D2 medium spiny neurons by cocaine and morphine. *bioRxiv [Preprint]*. https://doi.org/10.1101/2023.09.19.558477

Centers for Disease Control and Prevention. (2020). *Underlying Cause of Death, 1999-2020 Request.* https://wonder.cdc.gov/ucd-icd10.html

Counotte, D. S., Schiefer, C., Shaham, Y., & O'Donnell, P. (2013). Time-dependent decreases in nucleus accumbens AMPA/NMDA ratio and incubation of sucrose craving in adolescent and adult rats. *Psychopharmacology, 231*(8), 1675–1684. https://doi.org/10.1007/s00213-013-3294-3

Eagle, D. M., Wong, J. C. K., Allan, M. E., Mar, A. C., Theobald, D. E., & Robbins, T. W. (2011). Contrasting Roles for Dopamine D1 and D2 Receptor Subtypes in the Dorsomedial Striatum but Not the Nucleus Accumbens Core during Behavioral Inhibition in the Stop-Signal Task in Rats. *The Journal of Neuroscience, 31*(20), 7349–7356. https://doi.org/10.1523/jneurosci.6182-10.2011

Encyclopedia of DNA Elements. (2018, July 16). *Data Production and Processing Standard of the Hi-C Mapping Center.* https://www.encodeproject.org/documents/75926e4b-77aa-4959-8ca7-87efcba39d79/@@download/attachment/comp_doc_7july2018_final.pdf

Godino, A., Salery, M., Durand-de Cuttoli, R., Estill, M. S., Holt, L. M., Futamura, R., Browne, C. J., Mews, P., Hamilton, P. J., Neve, R. L., Shen, L., Russo, S. J., & Nestler, E. J. (2023). Transcriptional control of nucleus accumbens neuronal excitability by retinoid X receptor alpha tunes sensitivity to drug rewards. *Neuron, 111*(9), 1453–1467.e7. https://doi.org/10.1016/j.neuron.2023.02.013

Grubert, F., Srivas, R., Spacek, D. V., Kasowski, M., Ruiz-Velasco, M., Sinnott-Armstrong, N., Greenside, P. G., Narasimha, A., Liu, Q., Geller, B., Sanghi, A., Kulik, M., Sa, S., Rabinovitch, M., Kundaje, A., Dalton, S., Zaugg, J. B., & Snyder, M. (2020). Landscape of cohesin-mediated chromatin loops in the human genome. *Nature, 583*(7818), 737–743. https://doi.org/10.1038/s41586-020-2151-x

Hansen, A. S., Cattoglio, C., Darzacq, X., & Tjian, R. (2017). Recent evidence that TADs and chromatin loops are dynamic structures. *Nucleus, 9*(1), 20–32. https://doi.org/10.1080/19491034.2017.1389365

Kadauke, S. & Blobel, G. A. (2009). Chromatin Loops in Gene Regulation. *Biochimica et Biophysica Acta (BBA) - Gene Regulatory Mechanisms*, *1789*(1), 17–25. https://doi.org/10.1016/j.bbagrm.2008.07.002

Lin, D., Sanders, J., & Noble., W. S. (2021). HiCRep.py: fast comparison of Hi-C contact matrices in Python. *Bioinformatics, 37*(18), 2996–2997. https://doi.org/10.1093/bioinformatics/btab097

Mews, P., Walker, D. M., & Nestler, E. J. (2018). Epigenetic Priming in Drug Addiction. *Cold Spring Harbor Symposia on Quantitative Biology, 83*, 131–139. https://doi.org/10.1101/sqb.2018.83.037663

National Institute on Drug Abuse (2021, July 9). *What are the long-term effects of cocaine use?.* https://nida.nih.gov/publications/research-reports/cocaine/what-are-long-term-effects-cocaine-use

New England BioLabs. (2022). *NEBNext Ultra II DNA Library Prep Kit for Illumina*. https://www.neb.com/en-us/-/media/nebus/files/manuals/manuale7103-e7645.pdf?rev=de09eaf8fcdf45e0ac8a66bf6fee75fb&hash=346DB0B0FD1203244DC01FBEAFA2D259

Soares-Cunha, C., Coimbra, B., Domingues, A. V., Vasconcelos, N., Sousa, N., & Rodrigues, A. J. (2018). Nucleus Accumbens Microcircuit Underlying D2-MSN-Driven Increase in Motivation. *ENeuro, 5*(2), ENEURO.0386-18.2018. https://doi.org/10.1523/eneuro.0386-18.2018

Venton, B. J., Seipel, A. T., Phillips, P. E., Wetsel, W. C., Gitler, D., Greengard, P., Augustine, G. J., & Wightman, R. M. (2006). Cocaine increases dopamine release by mobilization of a synapsin-dependent reserve pool. *The Journal of Neuroscience*, *26*(12), 3206–3209. https://doi.org/10.1523/JNEUROSCI.4901-04.2006